

Supporting materials

Visualization of Macrophage Recruitment to Inflammation Lesions using Highly Sensitive and Stable Radionuclide-Embedded Gold Nanoparticles as a Nuclear Bio-Imaging Platform

Sang Bong Lee^{1,2*}, Ho Won Lee^{1*}, Thoudam Debraj Singh¹, Yinghua Li³, Sang Kyoong Kim⁹, Sung Jin Cho⁴, Sang-Woo Lee^{1,2}, Shin Young Jeong¹, Byeong-Cheol Ahn¹, Sangil Choi⁵, In-Kyu Lee^{2,6}, Dong-Kwon Lim⁷✉, Jaetae Lee^{1,8}✉, Yong Hyun Jeon^{2,9}✉

1. Department of Nuclear Medicine, Kyungpook National University Hospital, Daegu, South Korea;
2. Leading-edge Research Center for Drug Discovery and Development for Diabetes and Metabolic Disease, Kyungpook National University Hospital, Daegu, South Korea;
3. Department of Pathology, Chemon Co. Ltd., 240, Nampyeong-Ro, Yangji-Myeon, Cheoin-Gu, Yongin-Si, Gyeonggi-Do, 17162, Republic of Korea;
4. New Drug Development Center, Daegu-Gyeongbuk Medical Innovation Foundation, Daegu, South Korea;
5. Department of Pharmacy, School of Pharmacy, Massachusetts College of Pharmacy and Health Sciences, Boston, Massachusetts, USA;
6. Department of Internal Medicine, Kyungpook National University School of Medicine, Deagu 700-721, South Korea;
7. KU-KIST Graduate School of Converging Science and Technology, Korea University, Seoul Anam-ro 145, South Korea;
8. Daegu-Gyeongbuk Medical Innovation Foundation, Daegu, South Korea;
9. Laboratory Animal Center, Daegu-Gyeongbuk Medical Innovation Foundation, Daegu, South Korea.

*The first two authors contributed equally to this study.

✉ Corresponding authors: Yong Hyun Jeon (jeong9014@gmail.com), Jaetae Lee (jaetae@knu.ac.kr), and Dong-Kwon Lim (dklim@korea.ac.kr).

Methods

Animals.

Specific pathogen-free, 6-week-old immunocompetent C57BL/6 mice were obtained from SLC, Inc. (Shizuoka, Japan). All animal experimental procedures were conducted in strict accordance with the appropriate institutional guidelines for animal research. The protocol was approved by the Committee on the Ethics of Animal Experiments of the Kyungpook National University (permit number: KNU 2012-43).

Materials.

Citrate-stabilized gold nanoparticles were purchased from Ted Pella, Inc. (Redding, CA). All other chemical reagents (HAuCl₄•3H₂O, dithiothreitol, DTT) were purchased from Sigma-Aldrich (St. Louis, MO), and used without further purification. Thiolated oligonucleotides were purchased from IDT Inc. (Coralville, IA) and reduced by using 0.1 M DTT in 0.17 M phosphate buffer (PB, pH = 8.0). The reduced oligonucleotides were then purified through a desalting NAP-25 column (Sephadex G-25 medium, DNA grade). NANO pure H₂O (>18.0 M), purified using a Milli-Q water purification system (Millipore, Billerica, MA), was used for all experiments. The precursor sulfosuccinimidyl-3-[4-hydroxyphenyl] propionate (SHPP) was purchased from Thermo Scientific (Rockford, IL). The radioisotope sodium iodide 124 (Na¹²⁴I) was provided by Duchem Bio (Daegu, South Korea), and KIRAMS (Seoul, South Korea). The chloramine-T hydrate was purchased from Sigma Aldrich. RPMI media, fetal bovine serum (FBS; Hyclone, Logan, UT) and media components (Hyclone) were used for cell culture. Carrageenan (Sigma Aldrich) was also purchased. Phycoerythrin (PE)-conjugated anti-CD86, CD11b, and fluorescein isothiocyanate (FITC)-conjugated anti-F4/80 were purchased from BD Biosciences (San Jose, CA).

Synthesis of RIe-AuNPs.

Citrate-modified gold nanoparticles were modified with thiolated adenine-rich oligonucleotides (3'-HS-(CH₂)₃-A10-5') using standard salt aging procedures.[17] For radioisotope labeling, the amine groups of the adenine base on the AuNPs (A10-AuNPs) were covalently conjugated with sulfo-SHPP, then reacted with radioactive sodium iodide (Na¹²⁴I or ¹²⁵I) in the presence of chloramine-T (Fig. S1). Briefly, 20 mL of A10-AuNP solution was reacted with sulfo-SHPP (1.0 mg) for 12 hours at room temperature and centrifuged to remove excess sulfo-SHPP (12,000 rpm/15 minutes), then the precipitates were redispersed in distilled water (20 mL). For radioisotope labeling during RI-AuNP preparation, 150 μL of Na¹²⁴I or ¹²⁵I (81.4 MBq), 90 μL of chloramine-T (3 mg/mL), and 100 μL of 1% sodium dodecyl sulfate were added into the SHPP-AuNP solution (1.0 mL of 1.0 nM) and gently shaken for 2 hours at room temperature. After centrifugation (12,000 rpm/15 min), the supernatant was removed and the precipitates were redispersed in distilled water (1.0 mL). The decay-corrected radiochemical yield was found to be over 90%. Finally, to prepare radionuclide-embedded gold nanoparticles (RIe-AuNPs), 1.0 mL of RI-AuNPs (1.0 nM) was mixed with 500 μL of 1.0% (w/v) poly(N-vinyl-2-pyrrolidone) solution (Mw 40 kDa), 100 μL of 100 mM phosphate buffer (pH 7.4), and 165 μL of 2.0 M NaCl. The reducing agent (434 μL of hydroxylamine hydrochloride (10 mM in distilled water)) was added and then 434

μL of HAuCl_4 (5 mM in distilled water) solution was quickly added and mixed very rapidly. The reaction mixtures were allowed to stand for 2 hours at room temperature and then purified by centrifugation (6,000 rpm/15 min). The supernatant was removed and the precipitates were redispersed in distilled water (1 mL). We calculated the loading number of radioisotopes per AuNP according to the information for the specific activity of ^{125}I provided by PerkinElmer Inc. (Waltham, MA) and the optical density measurement of the AuNP concentration. The observed specific activity of ^{125}I from 1.0 mL of AuNPs (OD = 1.0 at 520 nm) was 3.5 mCi (equivalent to 0.001609 mmol); therefore, the number of iodine molecules per AuNP was calculated to be 2681.

Phagocytic activity assay

The phagocytic activity of macrophage was measured using 7-aminoactinomycin D (7-AAD, BD Biosciences, Pharmingen)-stained *Escherichia coli* and fluorescence-activated cell sorting (FACS) analysis. *E. coli* (1×10^8 cells in 1 mL PBS) were incubated at 60°C for 1 hour for sterilization, and 1 mL of sterilized *E. coli* was further co-incubated with 50 μL 7-AAD for 2 hours at room temperature. For the opsonization of *E. coli* to allow phagocytosis by the macrophages, 5 μL 7-AAD-stained *E. coli* was incubated with 1 μL human serum for 20 minutes at room temperature. Opsonized *E. coli* stained with 7-AAD were added to 2.5×10^5 of both unlabeled and labeled macrophages and incubated in 50 μL RPMI-1640 culture medium (Hyclone) containing 10% FBS for 1 hour at either 4°C or 37°C . After 1 hour of incubation, the samples were washed twice with cold PBS and the fluorescence was analyzed using flow cytometry (BD Biosciences). The phagocytic activity of each cell was expressed as the increase in the percentage of 7-AAD-positive unlabeled and labeled macrophages compared to the macrophages treated with non-stained *E. coli*.

Measurement of 1% CG-induced paw edema

All mice were randomly divided into three groups; Control, 100 mg/kg GSK5182, and 10 mg/kg DEX groups. All mice were subcutaneously injected with PBS and 1% CG into the left and right paws, respectively. Mice received either a single dose of 100 mg/kg GSK5182 or 10 mg/kg DEX post-inflammation induction. Paw edema was measured at 0 (as baseline, before inflammation induction), 6, and 24 hours post injection of PBS and 1% CG. The change of dorsoventral thicknesses of the middle portions of the hind paws were measured using a caliper as previously reported [1].

Quantitative Real-Time PCR analysis for pro-inflammatory cytokines

PBS and 1% CG were subcutaneously injected into the left and right paws of mice. After 6 hours, mouse paws were cut at the ankle joint and preserved at -80°C until further processing. Paw samples were homogenized using a tissue homogenizer. Total RNA was isolated from the hind paws with TRIzol (Invitrogen, Carlsbad, CA) according to the manufacturer's instructions. Approximately 2 μg of total RNA was converted to cDNA by using the High Capacity cDNA Reverse Transcription kit (Applied Biosystems, Foster City, CA). Real-time PCR was performed on a CFX96 Touch Real-Time PCR System (Bio-Rad, Hercules, CA) using SsoAdvanced Universal SYBR Green Supermix (Bio-Rad). The primer sequences used for real time PCR were as follows; for *Il1beta*: Forward (5'-AAG TTG ACG GAC CCC AAA AGA T-3') and reverse (5'-TGT TGA TGT GCT GCT GCG A-3'), *Il6*: Forward (5'-AGT TGC CTT CTT GGG ACT GA-3') and reverse (5'-TCC ACG ATT TCC

CAG AGA AC-3'), *Tnfa*: Forward (5'-ATC TTC TCA AAA TTC GAG TGA CAA-3') and reverse (5'-ACT TGG GCA GAT TGA CCT CAG-3'), *M36b4*: Forward (5'-ACC TCC TTC TTC CAG GCT TT-3') and reverse (5'-CTC CAG TCT TTA TCA GCT GC-3'). We performed two independent experiments for each reaction in triplicate. All samples were normalized to *M36b4*, which was used as a reference gene.

Histological analysis

All organs of interest such as the liver, spleen, kidney, and CG-or PBS-injected footpads were collected and incubated in fixative solution, followed by H&E staining for the evaluation of potential adverse effects by R1e-AuNPs.

***In vivo* PET/CT study**

For the PET/CT study, a 20-minute scan (tumor imaging) was performed using LabPET8 (TriFoil imaging, Waukesha, WI). For 18F-FDG PET/CT imaging, a 10-minute scan was performed using the same animal PET/CT instrument as described above. CT scans were conducted after the PET scan. PET images were reconstructed by 3D-OSEM iterative image reconstruction and the CT images were reconstructed using filtered back-projections. All mice were anesthetized using 1–2% isoflurane gas during imaging. PET images were co-registered with anatomical CT images using the 3D image visualization and analysis software VIVID (Gamma Medica-Ideas, Northridge, CA). To measure the uptake (%ID/cc) for the volumes of interest (VOIs), the VOIs from each image were manually segmented from co-registered CT images using VIVID, and the uptake in the region of interest was measured with VIVID software.

Statistical analysis

All data are expressed as the means \pm standard deviation (SD) from at least three representative experiments, and statistical significance was determined using an unpaired Student's test with GraphPad Prism 5. P-values of < 0.05 were considered statistically significant.

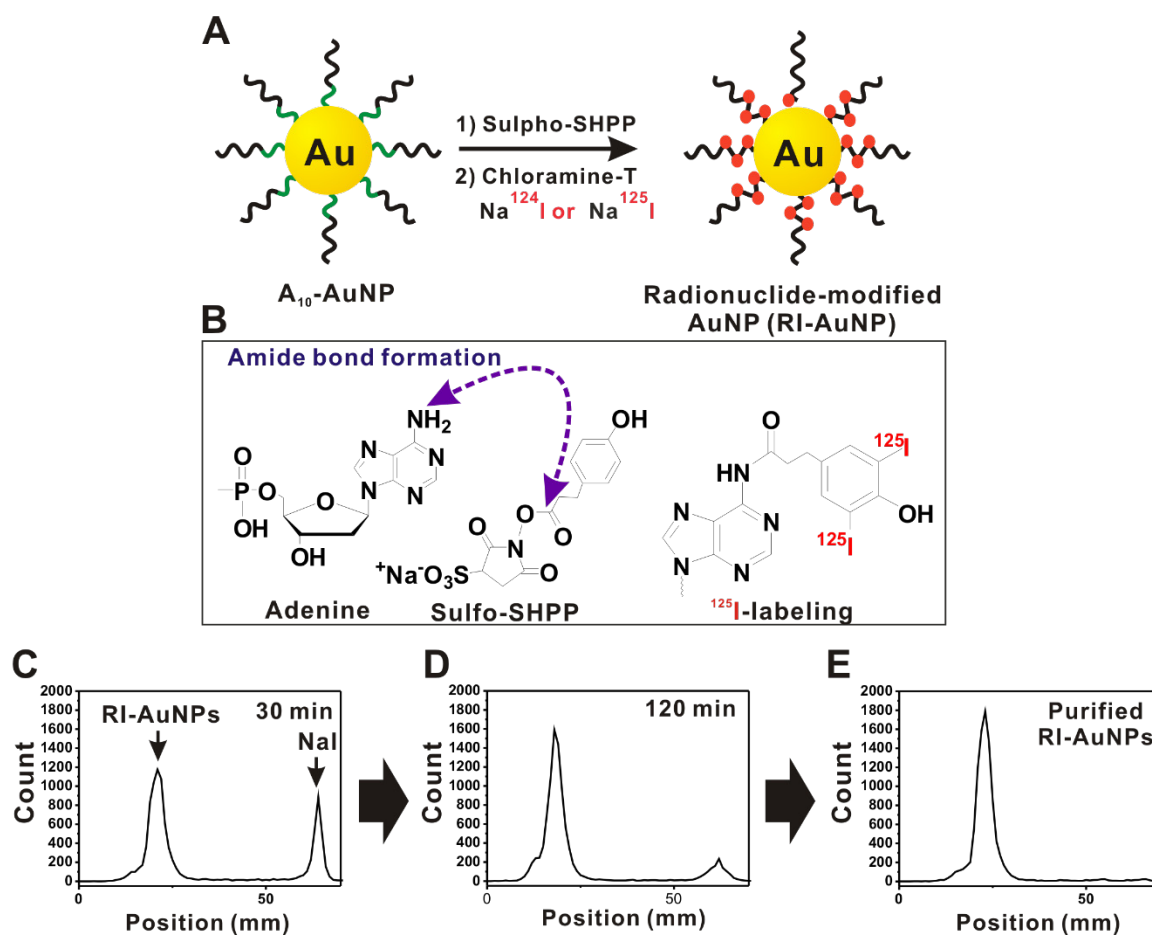


Figure S1. (A) Reaction scheme for radioiodine-modified AuNPs (RI-AuNPs). (B) Changes in the chemical structures of adenine with each reaction (Sulpho-SHPP and Na^{124}I and Na^{125}I). (C-E) Time-dependent chromatograms of thin layer chromatography to monitor the radiolabeling procedures.

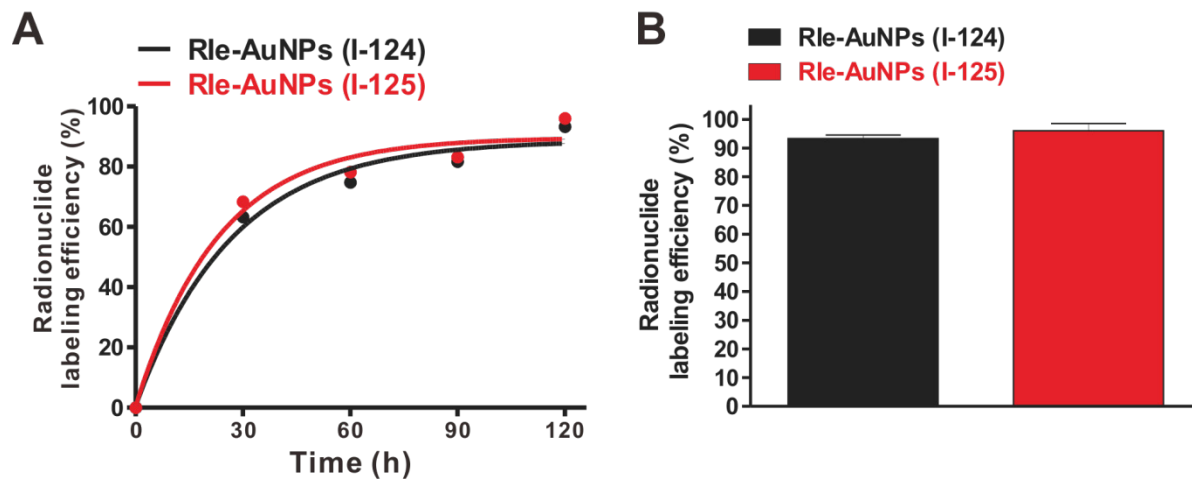


Figure S2. Labeling kinetics (a) and efficiency (b) of Na¹²⁴I and Na¹²⁵I on A₁₀-AuNPs

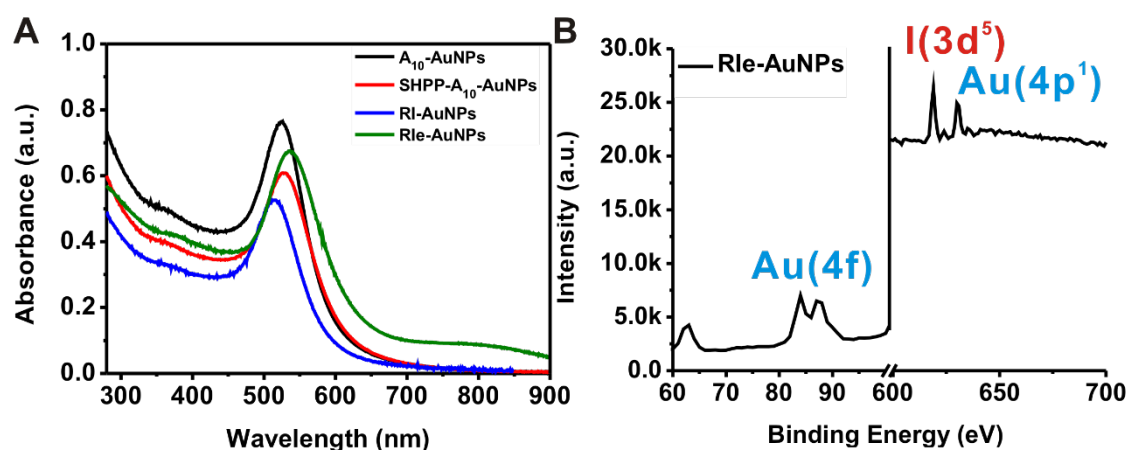
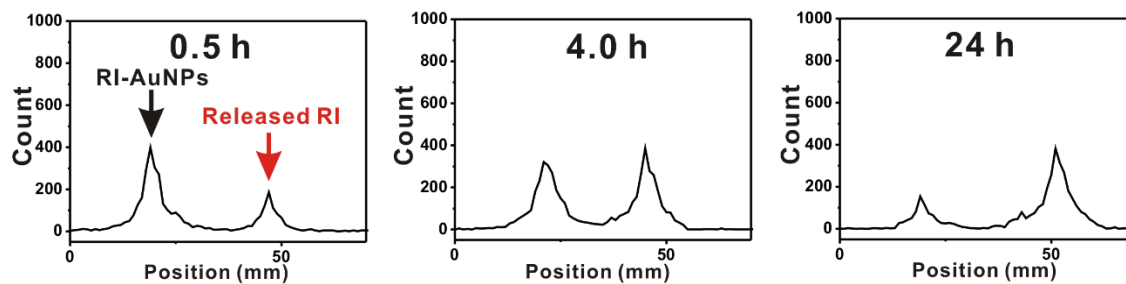


Figure S3. (a) UV-visible spectra of A₁₀-AuNPs, SHPP-A₁₀-AuNPs, RI-AuNPs (blue line), and radionuclide-embedded AuNPs (RIe-AuNPs, green line). (b) XPS data for RIe-AuNPs.

Stability of RI-AuNPs in human serum



Stability of RIe-AuNPs in human serum

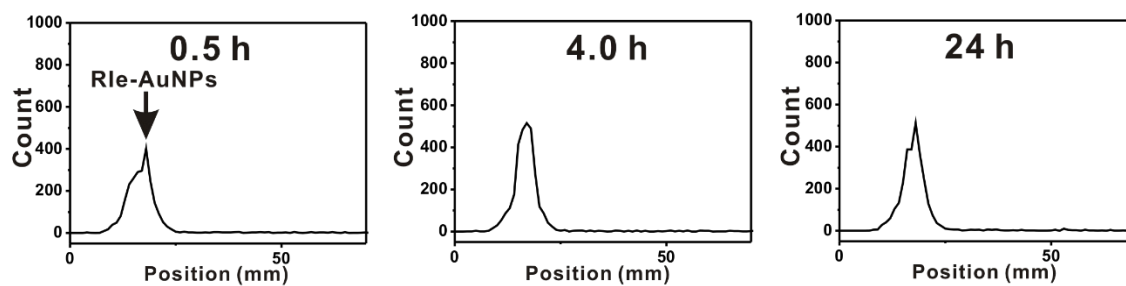


Figure S4. Time-dependent stability of RI-AuNP and RIe-AuNPs in human serum at 37°C.

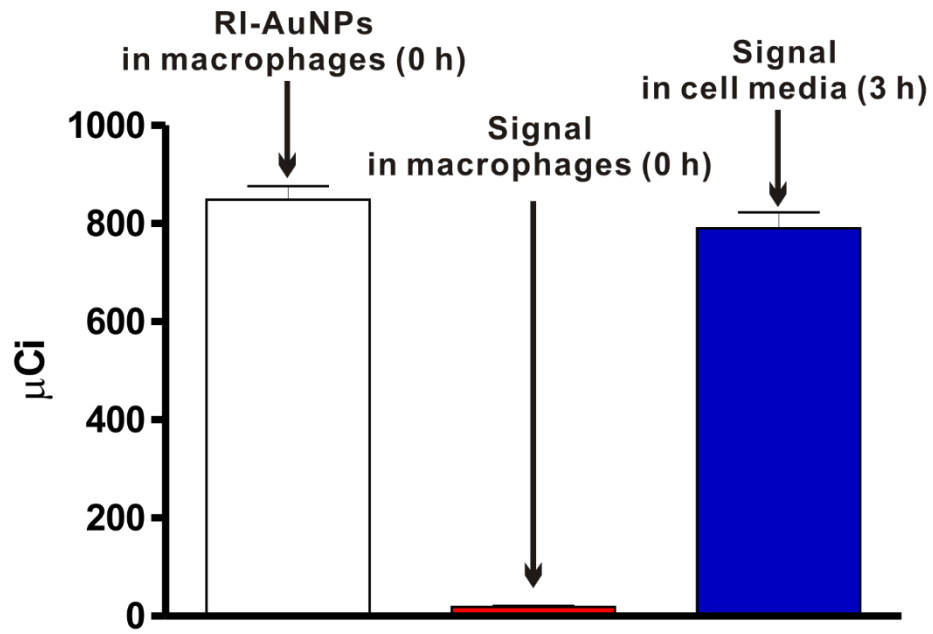


Figure S5. Radioactivity of macrophages labeled with RI-AuNPs and the changes of radioactivity in macrophages and cell media after 3 hours.

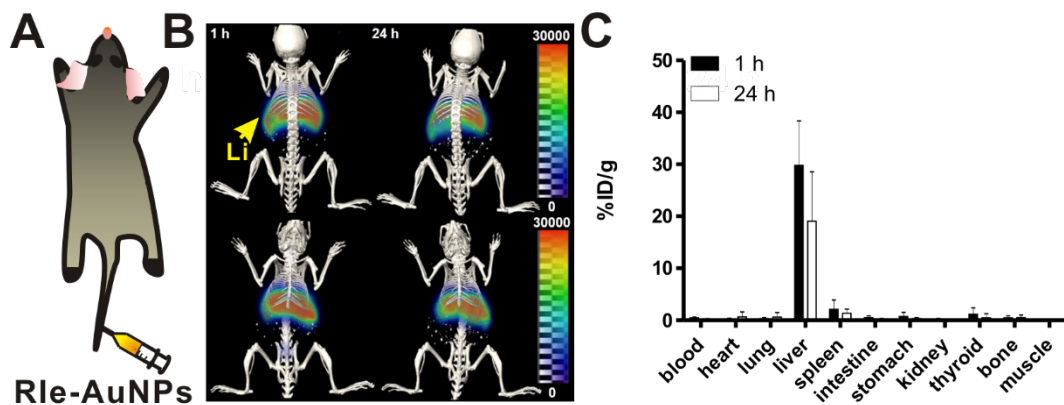


Figure S6. (a and b) 3D-constructed PET/CT images of intravenously injected RIe-AuNPs at 1 and 24 hours post-injection. Li: Liver (c) Relative organ-specific biodistribution of RIe-AuNPs at 1 and 24 hours after intravenous injection. Data are presented as the means \pm standard deviation. %ID/g = percentage injected dose per gram. Experiments were performed in triplicate (n = 5 mice per group).

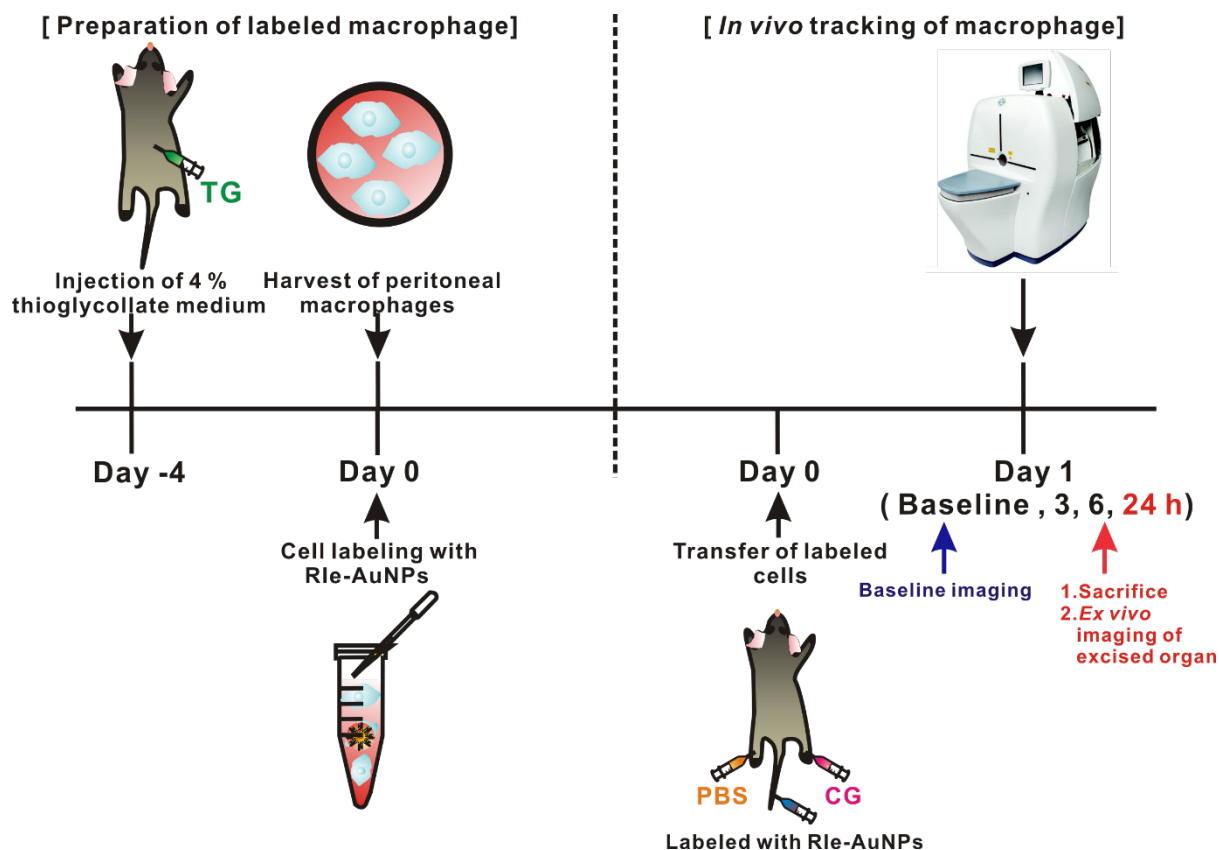


Figure S8. Protocols for *in vivo* animal experiments. Mice received 4% thioglycollate medium via intraperitoneal injection. After 3 or 4 days, 1×10^6 of peritoneal macrophages could be obtained per mouse. Isolated macrophages were labeled with 2 nM R1e-AuNPs for 3 hours and then the mice received labeled macrophages via the tail vein. Base line activity was acquired at 24 hours post-transfer and each mouse received either PBS or CG solution in the left and right footpad, respectively. The migration of labeled macrophages to the inflamed lesion was monitored by PET/CT at the indicated times. Mice were sacrificed and footpads were excised for *ex vivo* imaging.

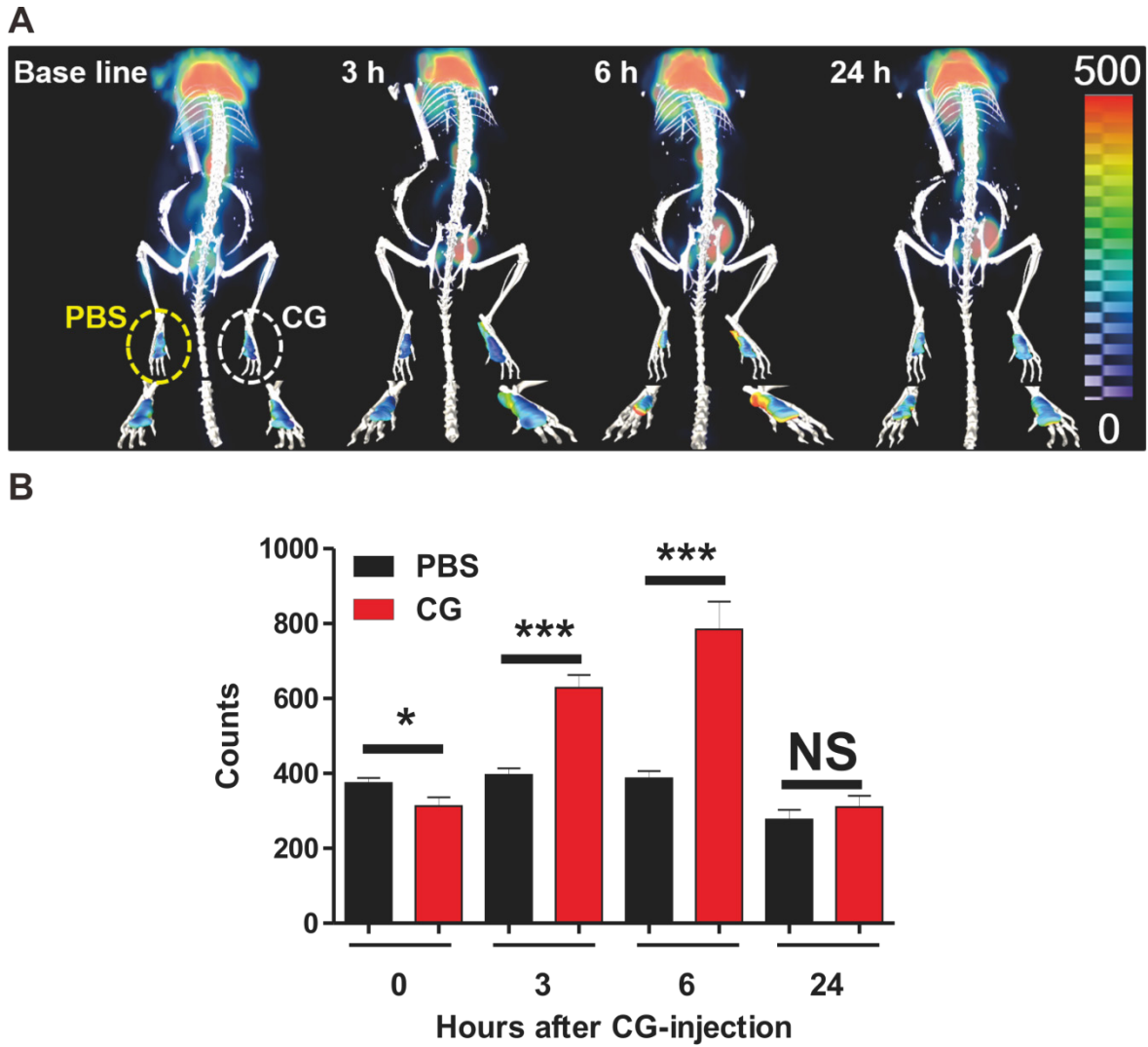


Figure S9. (a) F-18 FDG PET/CT imaging of mice with acute inflammation. Baseline activity was acquired with F-18 FDG PET/CT. Either PBS or CG solution was injected into the left and right footpad, respectively, and F-18 FDG PET/CT imaging was conducted at the designated times. (b) Quantification of FDG uptake in CG-injected footpads. The uptake value of CG-injected footpads was divided by that of PBS-injected footpads. * $P < 0.05$, *** $P < 0.001$. NS; not significant

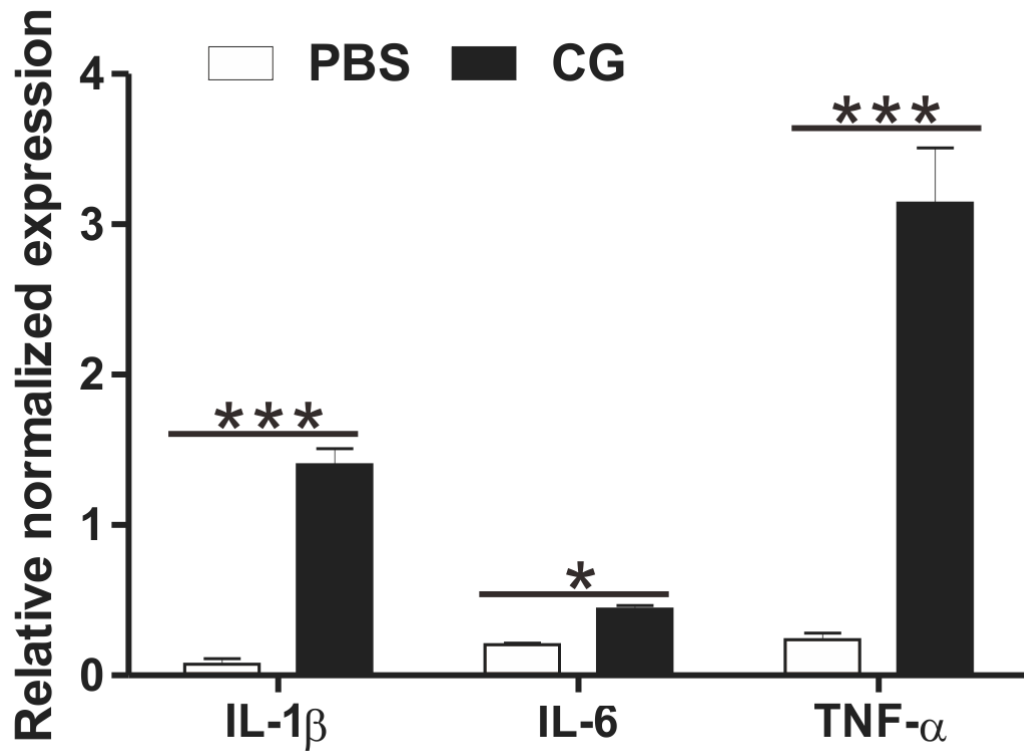


Figure S10. Levels of mRNA expression for IL- β , IL-6, and TNF- α in PBS- and CG-injected footpads. Total mRNA was prepared from each footpad and real-time PCR was performed to determine the mRNA expression level of the respective pro-inflammatory cytokines. * P < 0.05, *** P < 0.001.

Time (h) after CG-injection

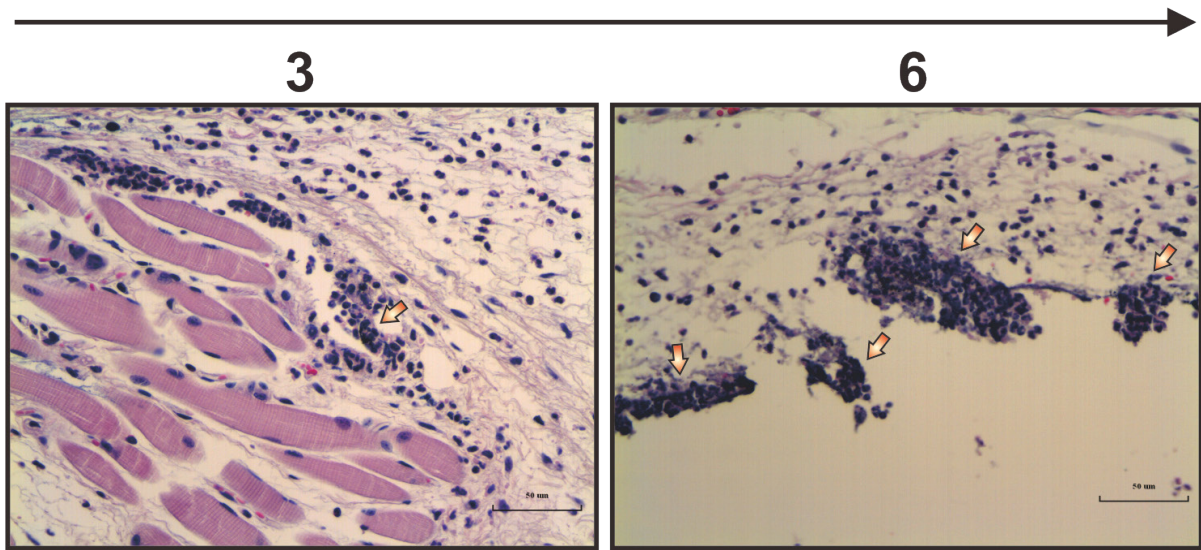


Figure S11. H&E staining in CG-injected footpads. White arrows indicate the gold particle-containing macrophages.

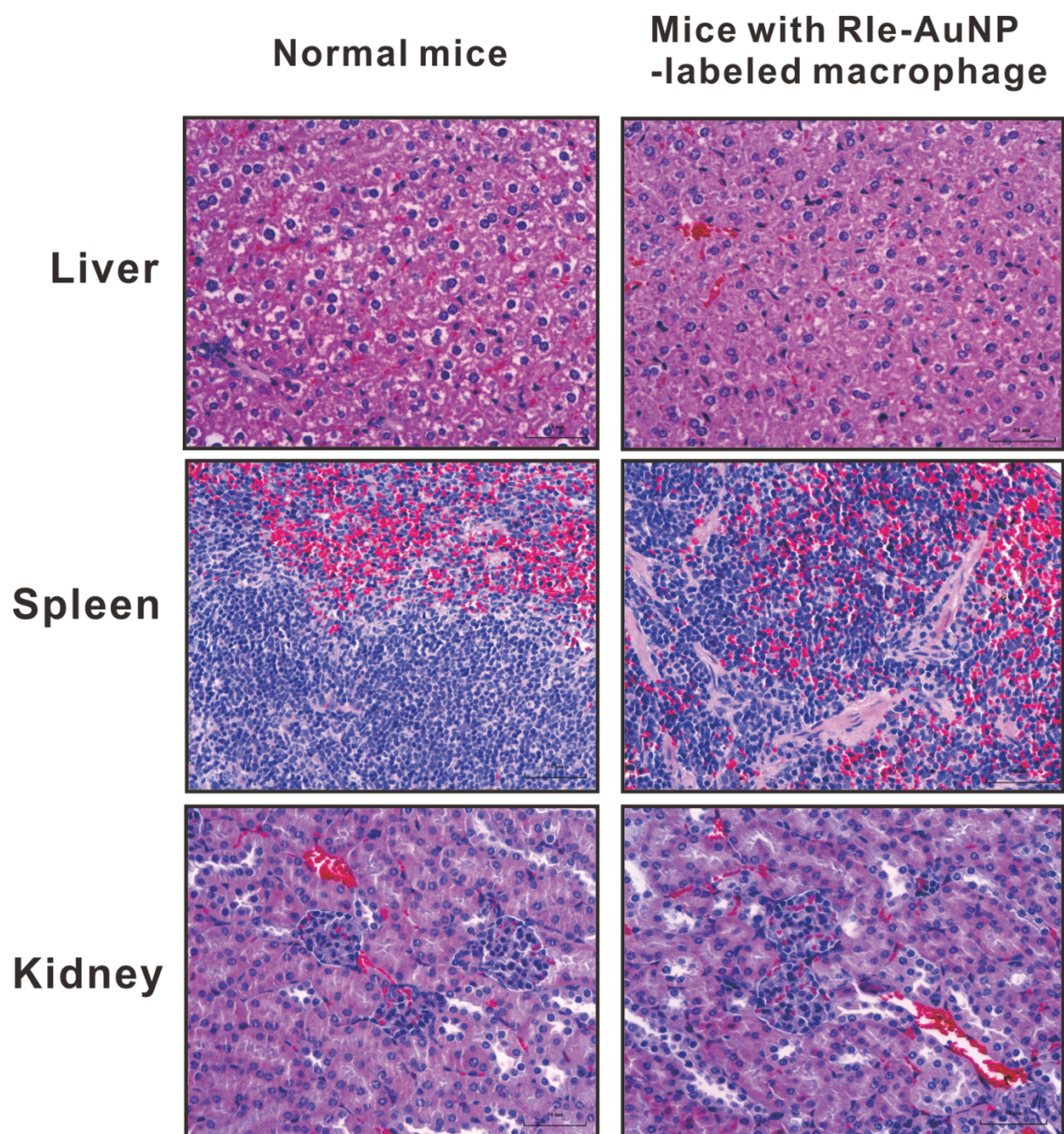


Figure S12. H&E stained images of the liver, spleen, and kidney in either normal mice or mice receiving RIe-AuNPs-labeled macrophages at 14 days after injection.

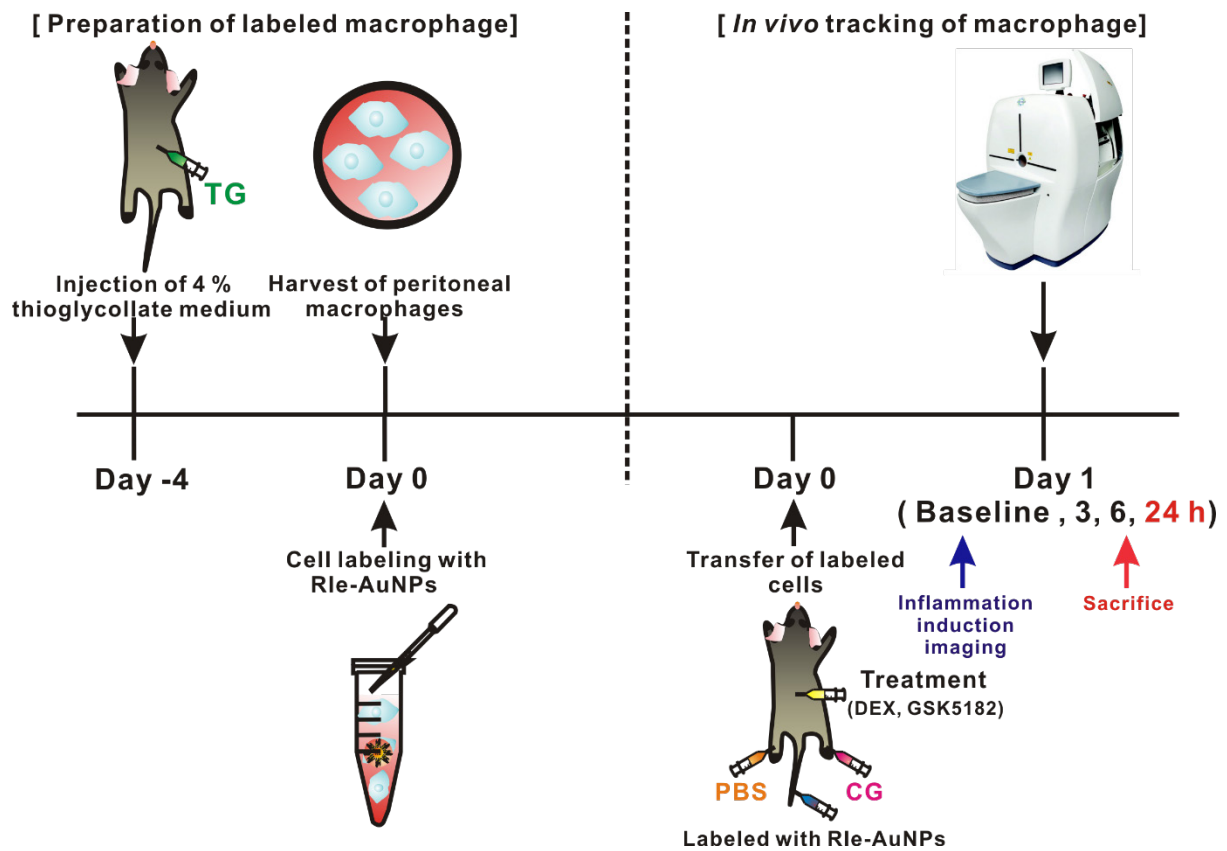


Figure S13. Schematic procedure for evaluation of the therapeutic efficacy of anti-inflammatory drugs *in vivo*. On day 1 post-transfer of labeled macrophages, mice were divided into three groups: vehicle group, DEX group, and GSK5182 group (n = 5 mice per group). Acute inflammation was generated using the same procedure as described above. Mice received either a single dose of 10 mg/kg DEX, GSK5182, or vehicle immediately after inflammation induction. PET was performed to monitor the migration of labeled macrophages at the indicated times.

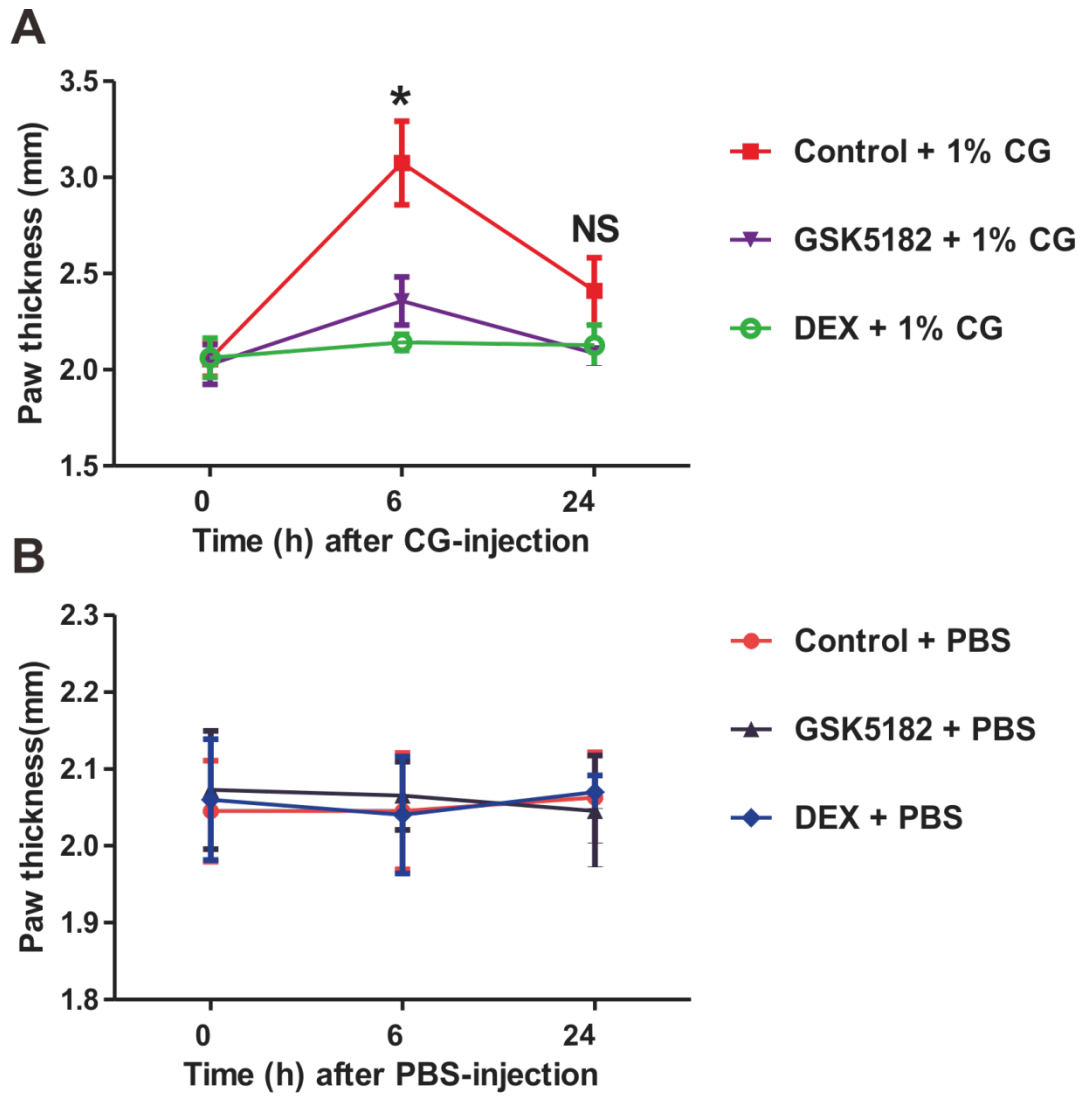


Figure S14. Measurement of paw thickness after PBS- or CG-injection with or without treatment by DEX or GSK5182. The change of hind paw thickness was measured using a caliper at the designated times. * $P < 0.05$. NS; not significant

REFERENCES

1. Jha MK, Song GJ, Lee MG, Jeoung NH, Go Y, Harris RA, et al. Metabolic connection of inflammatory pain: pivotal role of a pyruvate dehydrogenase kinase-pyruvate dehydrogenase-lactic acid axis. *J Neurosci*. 2015; 35: 14353-69.